Wind Engineering Joint Usage/Research Center
FY2023 Research Result Report

Research Field: outdoor environment
Research Year: FY2023
Research Number:
Research Theme: Analysis of interaction between heat waves and urban heat islands based on local climate zone framework in hot and humid region

Representative Researcher: Qiong Li

Budget [FY2021]: 360,000Yen

*There is no limitation of the number of pages of this report.
*Figures can be included to the report and they can also be colored.
*Submitted reports will be uploaded to the JURC Homepage.

1. Research Aim

Climate change has led to frequent heat wave events, with high temperature records being continuously broken worldwide. This study, through heat wave zoning and heat wave risk assessment, constructs an overall framework for heat wave disaster prevention and control, providing a reference for improving urban heat wave early warning systems. Building on the framework for heat wave disaster prevention and control, the research further selects areas under high heat stress for practical observation. Through a three-day heat environment test, it investigates and analyzes the heat stress levels in high-density communities in Guangzhou during heat waves, exploring the main factors affecting high-density urban areas. Ultimately, this study provides a reference for improving urban heat wave early warning systems and also proposes planning and design methods for future transformation and resettlement of areas with high heat stress and high population density.

2. Research Method

2.1 Guangzhou heat wave risk evaluation

High-temperature heat waves are defined by the relative threshold method, and heat wave intensity is calculated by using the apparent heat wave magnitude index to compute characteristics such as the incidence and intensity of heat waves. The calculation of heatwave intensity follows the “Apparent heatwave Index” (AHWI) proposed by Russo et al. Quantifying heatwave magnitudes based on local historical events, the daily magnitude (Md) was calculated as follows:

$$M_d = \begin{cases} \dfrac{T_d - T_{61y25p}}{T_{61y75p} - T_{61y25p}}, if\ T_d > T_{61y25p}\ and\ T \geq AT \\ \dfrac{AT_d - T_{61y25p}}{T_{61y75p} - T_{61y25p}}, if\ T_d > T_{61y25p}\ and\ T < AT \\ 0, if\ T_d \leq T_{61y25p} \end{cases}$$

Mann-Kendall trend detection method with sen's slope estimator is used to calculate the heat wave trend. The spatial hierarchical clustering method is used to divide the high-temperature heat wave zoning, and the trend indicator is used as one of the zoning bases to provide scenario categorization for the study of urban thermal environments in extreme hot weather.

On the basis of Crichton's risk triangle theory, a high-temperature heat wave hazard-exposure-vulnerability evaluation index system was developed, ten vulnerability assessment indicators were aggregated by principal component analysis, and the integrated high-temperature heat wave risk was calculated based on the multiplication rule to establish a heat wave risk map for the main urban area of Guangzhou City.

2.2 On-site thermal environments measurement

The test selects Changban community as the primary study area (Figure 1). As an old urban area in Guangzhou, the Changban community comprises three distinct residential zones with significant differences. Past urban management and planning efforts have targeted the transformation of new residential areas.

Due to the complex local traffic conditions, fixed observation points are easily affected by pedestrians and vehicles. Therefore, this thermal environment observation adopts a mobile observation method. The measuring instrument will be mounted on an electric vehicle, and a complete observation will record the air temperature and relative humidity of three types of residential areas and parks. Meteorological station data will be used to correct the mobile observation data to ensure data accuracy and reliability.

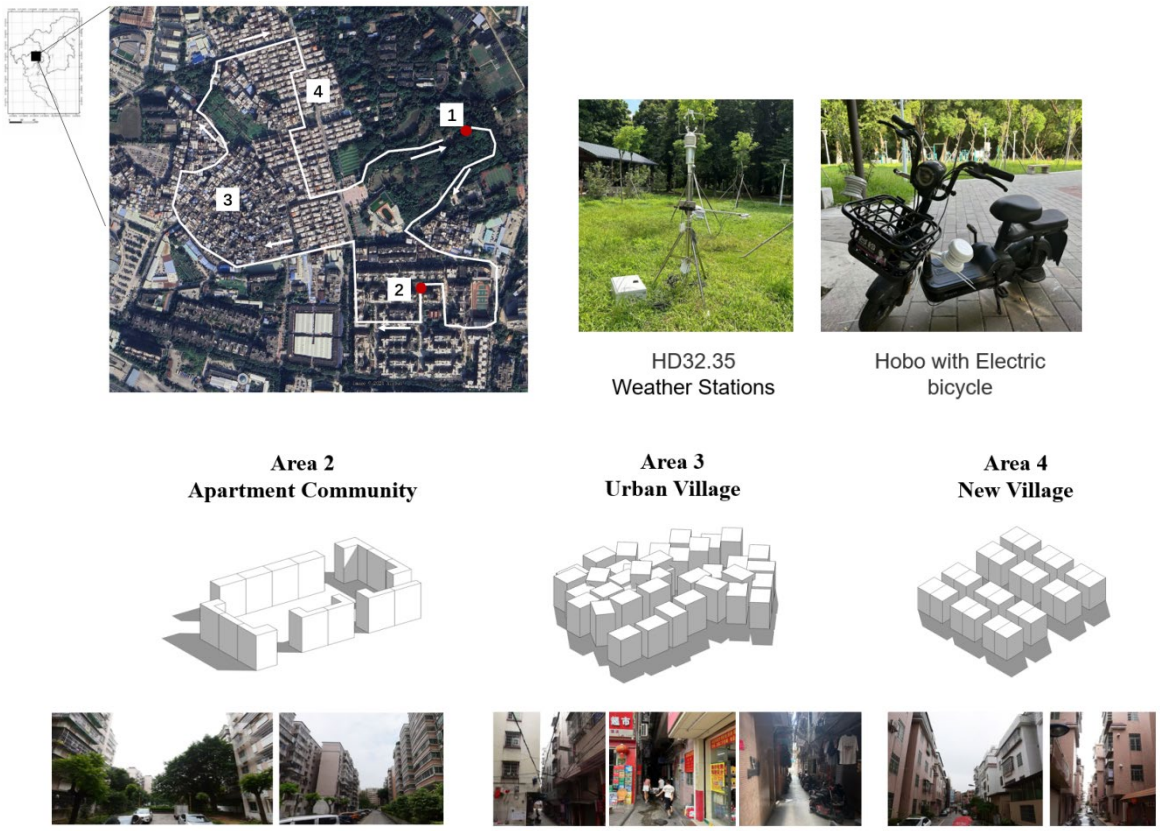

Figure 1 Measurement routes and meteorological stations(red point).

A single complete measurement was constrained to a duration of 20 minutes. Measurement was conducted hourly from 8:30 am to 8:30 pm. The vehicle maintains a constant speed of 2 m/s, and the Hobo sensor's height was set at 1.1 meters and entire observational route spans a length of 3.8 kilometers.

3. Research Result

3.1 Multi-level heat wave regionalization.

3.1.1 Zoning parameters and zoning result

Four climatic regions with significant trends (WAS, SW, C, and S regions) were selected for mutation detection. Figure 2 shows a clear tendence which all regions' trends mutate around 2000, and the stable sequence after this node is more representative. Therefore, the average heatwave characteristics from 2001 to 2021 and the 61-year trend of heatwave characteristics are selected as indicators.

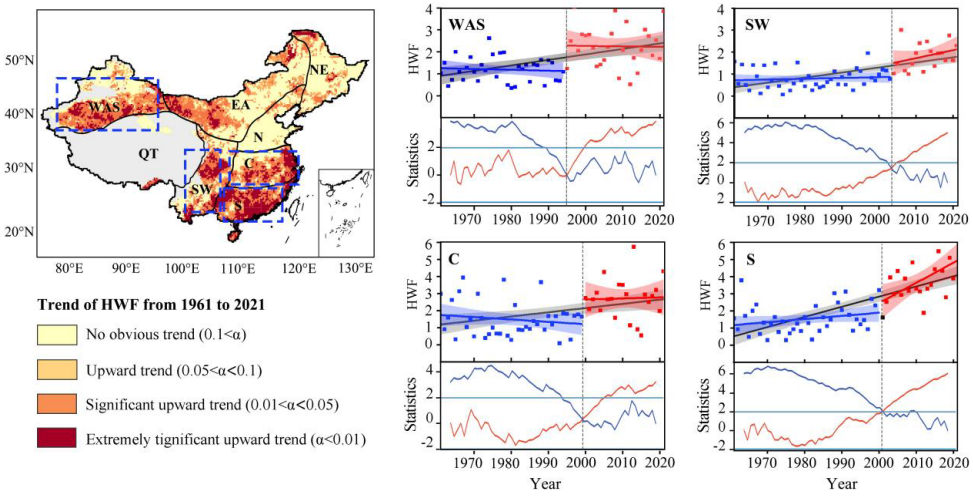

Figure 2 The right figure shows the distribution of Z-value of HWF from 1961 to 2021, the left graph shows the Scatter plot and M-K mutation test chart of the annual heatwave frequency in WAS, SW, C, and S regions. Among them, in the scatter plot, the shading represents the 95% confidence level; in the M-K mutation test chart, the blue and red curves are UBk statistics and UFk statistics, blue horizontal lines represent 2 confidence lines of α = 0.05, the intersection point of the UBk curve and the UFk curve between the confidence lines is the mutation point, the gray vertical lines mark the point of abrupt change.

Fig. 3 illustrates China's heatwave characteristic zones map from 2001 to 2021. The right graph in Fig.3 shows the distribution of Z-value of HWF from 1961 to 2021, the left graph shows the Scatter plot and M-K mutation test chart of the annual heatwave frequency in WAS, SW, C, and S regions. Among them, in the scatter plot, the shading represents the 95% confidence level; in the M-K mutation test chart, the blue and red curves are UBk statistics and UFk statistics, blue horizontal lines represent 2 confidence lines of α = 0.05, the intersection point of the UBk curve and the UFk curve between the confidence lines is the mutation point, the gray vertical lines mark the point of abrupt change.

the distribution of HWD and HWF is highly consistent in geographical space. Areas with high frequency of heatwaves often correspond to larger annual cumulative days. It can be considered that the average duration of a single heatwave event in most areas have little difference. The frequency of heatwaves have significant geographical features, basically showed a decreasing trend from south to north. The regions with the highest incidence are South China coastal area, with an average HWF of 2 to 5 times per year, and an average HWD of more than 10 days per year, followed by the middle and lower reaches of the Yangtze River, the Sichuan Basin and the Tarim Basin. And these high-value areas basically belong to plains and basins.

six zones representing typical heatwave characteristics were formed as shown in **エラー! 参照元が見つかりません。**3. They are, respectively, Low AT and Low Frequency (LALF), Moderate AT and Low Frequency (MALF), Moderate AT and Moderate Frequency (MAMF), High AT and Moderate Frequency with High Magnitude (HAMF-HM), High AT and Moderate Frequency with Moderate Magnitude (HAMF-MM), High AT and High Frequency (HAHF).

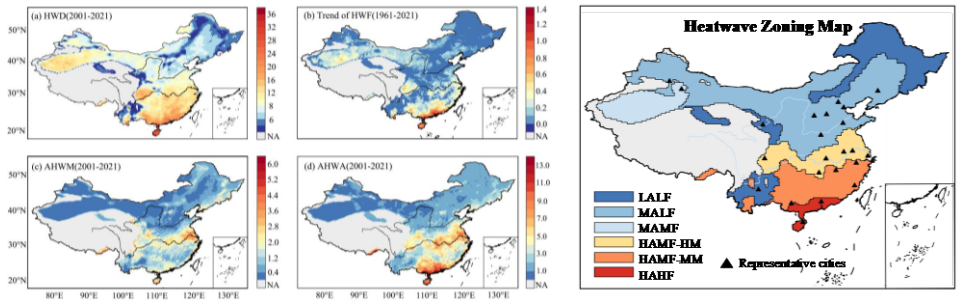

Figure 3 China's heatwave characteristic zones map from 2001 to 2021.The gray area has no heatwave, and the white area is the lack of meteorological data within the scope of China.

エラー! 参照元が見つかりません。4 shows the heatwaves characteristics of 6 zones and 24 major cities located in each sub-zone. The representative cities are mainly capital cities whose urban area are mainly located in certain sub-zone. The study used T-test and ANOVA analysis to judge the significance of the differences among the zones. It can be found that the six sub-regions showed significant differences in the four heatwave parameters as a whole. Among them, HWD and trend of HWF are related to the incidence of heatwaves. HWD and the trends of HWF showed a synergistic change among different zones, indicating that areas with frequent heatwaves often face greater heatwaves growth risk (e.g. Haikou, Guangzhou, Hong Kong in HAHF).

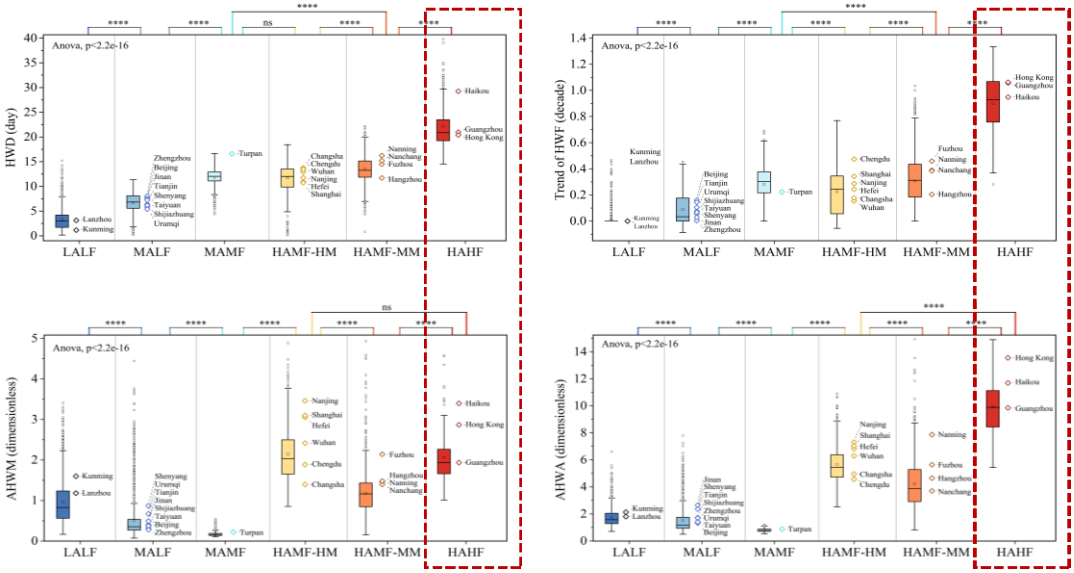

Figure 4 Distribution of HWD, AHWM, AHWA, and Trend of HWF in each of the zones. The difference between adjacent groups was judged by T test, *** represents the significance level of 0.05, **** represents the significance level of 0.01, “ns” represents the groups did not pass the significance test, and the ANOVA analysis was used to judge the significance level of each group, ANOVA analysis was used to judge the significance level of the differences among all the zones.

3.1.2 Characterization of heatwave in the urban area of Guangzhou

Guangzhou, a typical urban area in the HAHF zone, was selected as the assessment area. The region has a subtropical monsoon climate with a long duration of summer (May-October), with obvious hot and humid characteristics. The main urban area of Guangzhou City has a high density of buildings and population, and the living environment is extremely unbalanced. Some areas experience severe localized high temperatures due to the physical environment, while others are more vulnerable due to the socioeconomic factors. Figure 5 shows the basic geography information of research area.

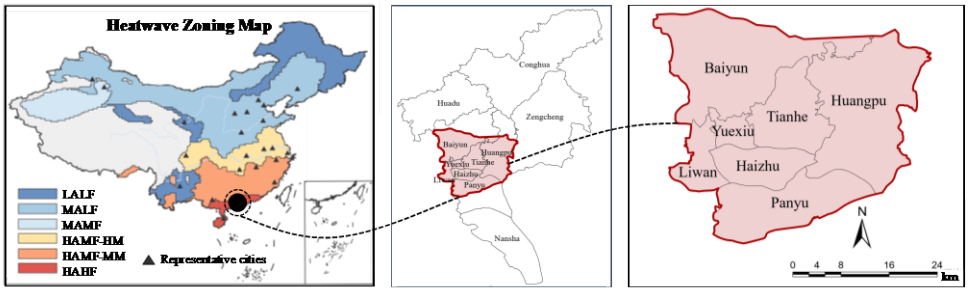

Figure 5 Research area

Through the collection and analysis of historical meteorological data, we have derived the Daily Threshold Distribution and the Time Series of Heat Wave Events spanning from 1961 to 2021 (as shown in Fig.6 and Fig.7). The high temperature threshold basically above 35°C in July and August, and lower in early summer while people have not yet experienced heat acclimatization. Heat waves in Guangzhou began to increase significantly around 2000. The frequency and intensity of heat waves have been

exceeding historical peaks since 2014, after a small decline from around 2009 to 2013.

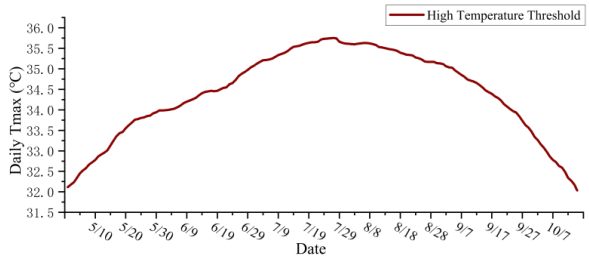

Figure 6 Daily Threshold Distribution in Guangzhou

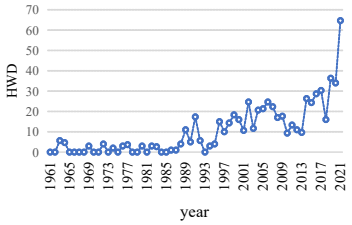

Figure 7 Time series of heat wave events in Guangzhou City over the years 1

3.2 Observation of thermal environment in high-risk region under heat wave events

Based on the heat wave risk zoning, this study conducted on-site measurements of typical neighborhoods to assess the thermal environment conditions of urban villages and new villages during a complete heat wave event. During heatwaves, the air temperature and relative humidity in route are shown in the Fig.8 and Fig.9. Different local areas exhibit significant spatiotemporal characteristics during heatwave events. The average air temperature and humidity (as shown in Fig.10 and Fig.11) at these four regions reflect the significant differences in local spatial heat environments. Apart from the spatial differences due to different locations, the heat environment varies with time and space, exhibiting distinct spatiotemporal characteristics.

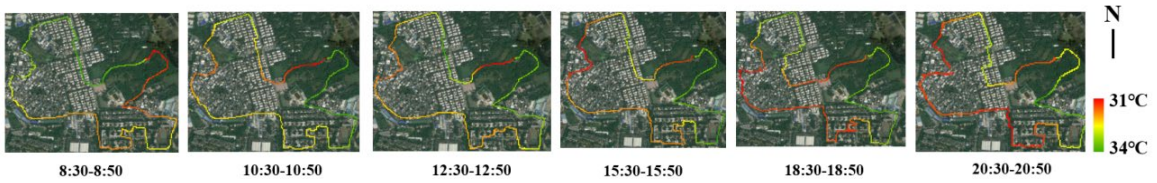

Figure 8 Average air temperature distributions along the mobile route in 5th August

Figure 9 Average relative humidity distributions along the mobile route in 5th August

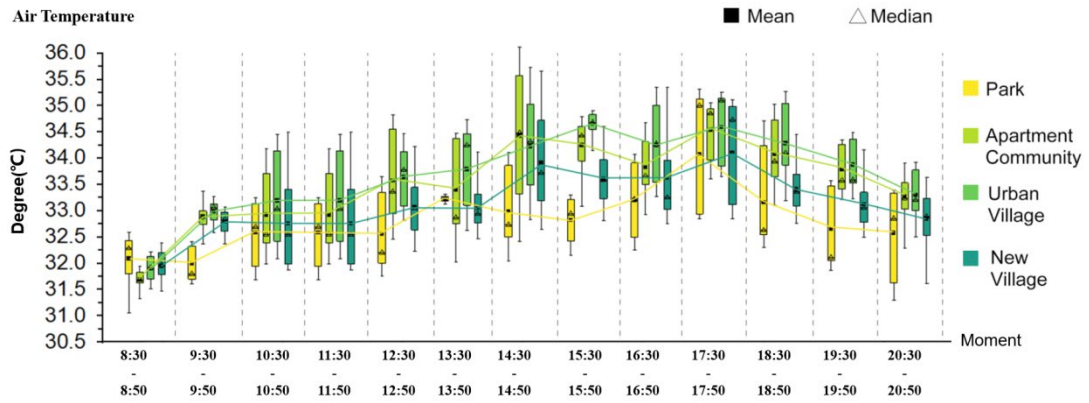

Figure 10 The distribution of air temperatures in four different types of regions under heat wave (5th-7th)

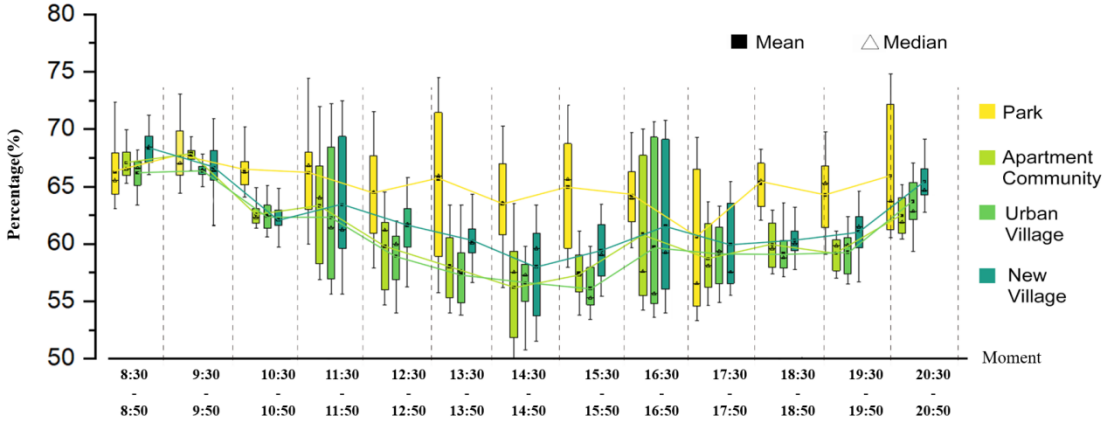

Figure 11 The distribution of relative humidity in four different types of regions under heat wave (5th-7th)

Based on the principle that the spatial distribution of urban spatial parameters tends to be continuous, this study utilized air relative humidity data from multiple mobile test points along a moving route. Using the spline function in spatial interpolation, spatial estimation calculations were performed to determine the distribution of the heat environment across the entire area. The comprehensive criteria reflected both accurately representing given data points and ensuring the smooth generation of spline functions. This method aligns well with relevant spatial analyses in local climate research. This integrated criterion reflects the dual objectives of accurately representing the given data points and ensuring the smoothness of the resulting spline function. The calculation formula is as follows:

$$F(r) = T(r) + \sum_{j=1}^{N} \lambda_j R(r, r_j)$$

T(r) represents the trend function, R(r,rj) denotes the basis function.

Based on spatial interpolation calculation, the study obtained data on the overall air temperature distribution during heatwaves in the region. Fig 12 presents the distribution of partial air temperatures in three days. The image illustrates similar patterns of changes in air temperature throughout the day during the heatwave event. In the early morning, all three types of areas experience relatively low air temperatures. At noon, as temperatures rise, both urban villages and apartment communities witness a substantial increase in air temperatures, with some areas reaching 33°C. The new village area maintains the lowest temperature among the three types of regions, hovering around 31 degrees Celsius. During the night, as residents go outdoors, urban villages and residential areas continue to maintain relatively high air temperatures, with some areas reaching 32.3°C.

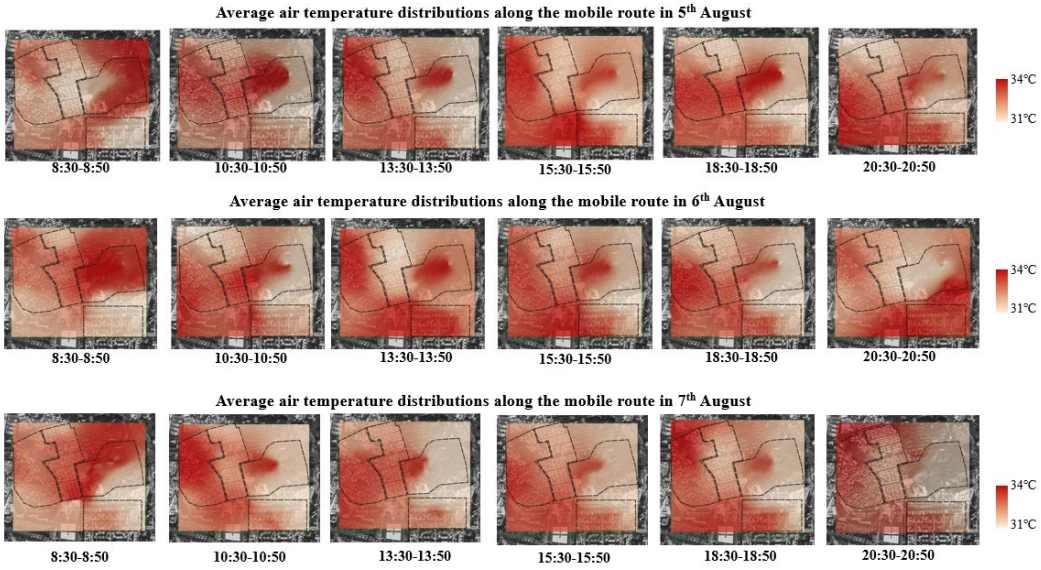

Figure 12 Air temperature distribution calculated by spatial interpolation method

Further, Researcher utilized the Heat Index to assess the thermal environment of two types of residential areas: urban villages and urban communities. The heat index (HI) is an index that combines air temperature and relative humidity, in shaded areas, to posit a human-perceived equivalent temperature. For high-density building areas, most of their interior spaces are consistently in shadow, making the Heat Index (HI) highly suitable for thermal stress. The equation and HI level is as follows:

$$HI = -42.379 + 2.04901523 * T + 10.14333127 * RH - .22475541 * T * RH - .00683783 * T * T - .05481717 * RH * RH + 0.00122874 * T * T * RH + .00085282 * T * RH * RH - .00000199 * T * T * RH * RH$$

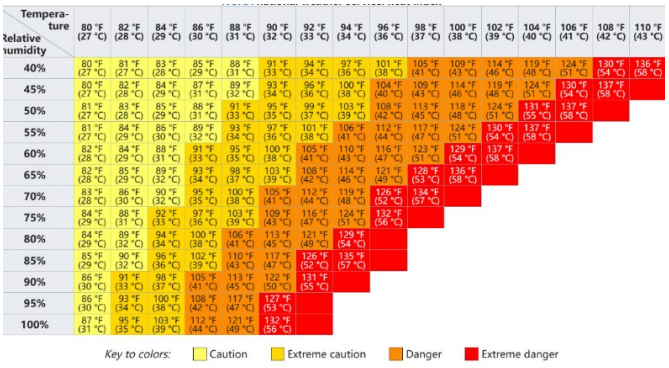

Heat Index	Heat Index Level
Less than 26.7 °C	Safe: no risk of heat hazard
26.7 °C - 32.2 °C	Caution: fatigue is possible with prolonged exposure and activity. Continuing activity could result in heat cramps.
32.2 °C - 39.4 °C	Extreme caution: heat cramps and heat exhaustion are possible. Continuing activity could result in heat stroke.
39.4 °C - 51.7 °C	Danger: heat cramps and heat exhaustion are likely; heat stroke is probable with continued activity.
over 51.7 °C	Extreme danger: heat stroke is imminent.

Figure 13 Heat index level

The spatial interpolation method was employed to derive the distribution of air temperature and relative humidity. Using the calculation formula for the Heat Index (HI), the entire region's Heat Index distribution and thermal stress situation during a heatwave event over three consecutive days were determined((as shown in Fig.14, Fig.15 and Fig.16).

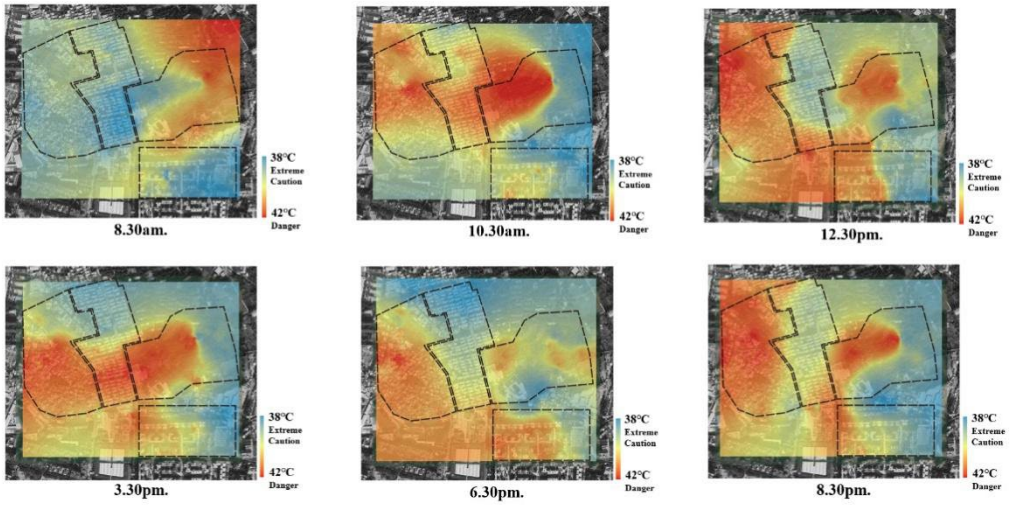

Figure 14 Thermal risk distribution by Heat Index(5th August)

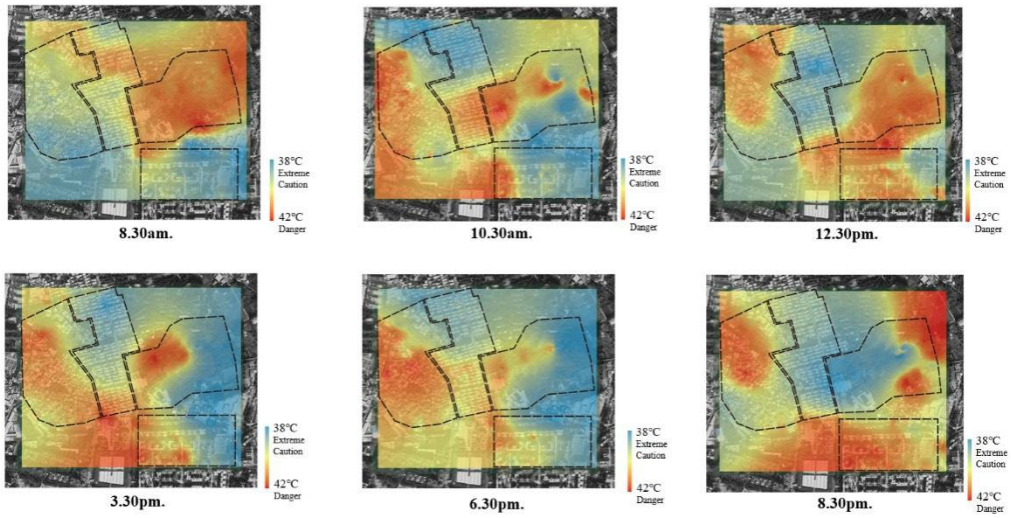

Figure 15 Thermal risk distribution by Heat Index(5th August)

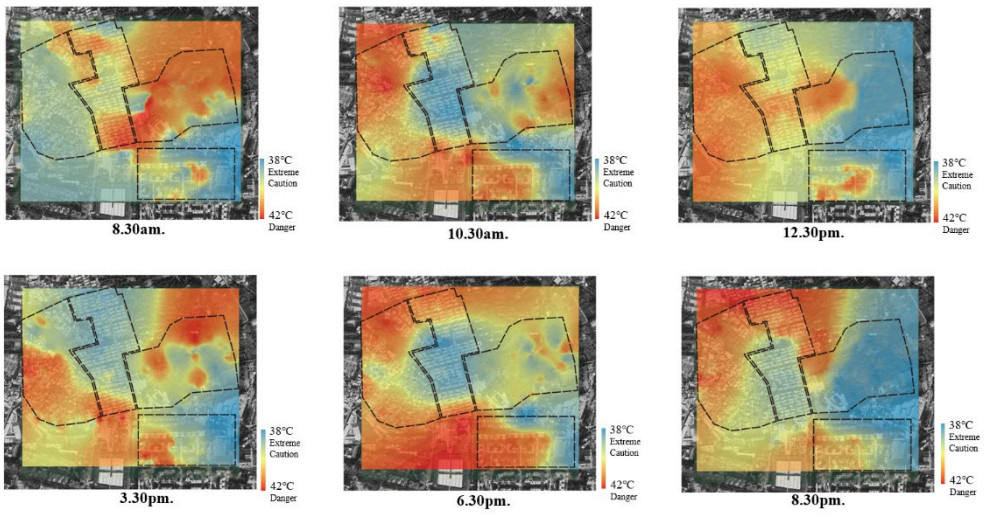

Figure 16 Thermal risk distribution by Heat Index(5th August)

As the intensity of the heatwave diminishes, there is an overall decreasing trend in the average Heat

Index within the region. The graphs（as shown in Fig.17，Fig.18 and Fig.19) illustrate that urban villages exhibit the highest Heat Index during the heatwave, reaching around 41°C at 3:00 PM and sunset. Even an hour after sunset, the average Heat Index remains very close to the danger level. The average Heat Index trend throughout the day in new villages and apartment communities is similar, but there are variations at different times of the day, primarily influenced by the thermal environment in urban villages. In terms of heat stress, all three types of residential areas experienced temperatures exceeding 40 degrees Celsius during the daytime of heatwave events. Urban villages had the most severe heat environment, with the Heat Index reaching the "dangerous" level for most of the daytime hours. Residents working outdoors in this area were at a high risk of heat-related issues. New villages and apartment communities had similar Heat Index values, providing a relatively safer outdoor heat environment in the morning but increasing heat risks as temperatures rose.

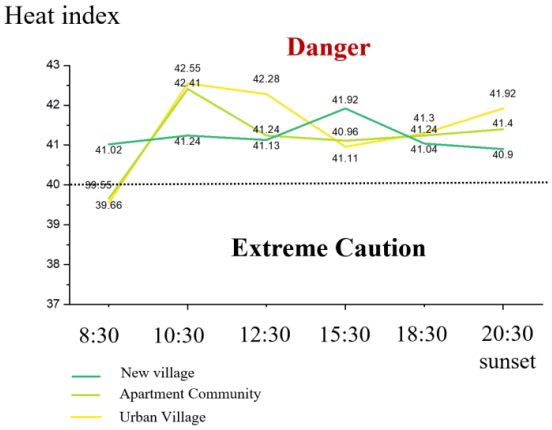

Figure 17Average heat index level in three residential areas in 5th Aug

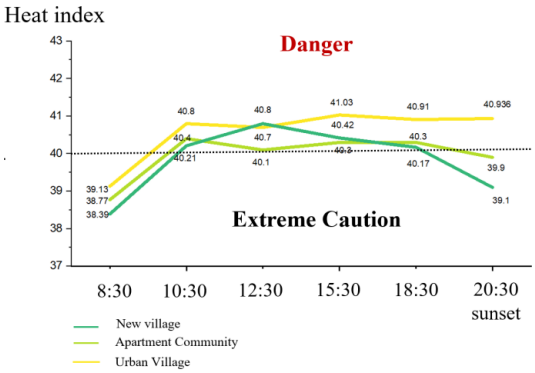

Figure 18 Average heat index level in three residential areas in 6th Aug

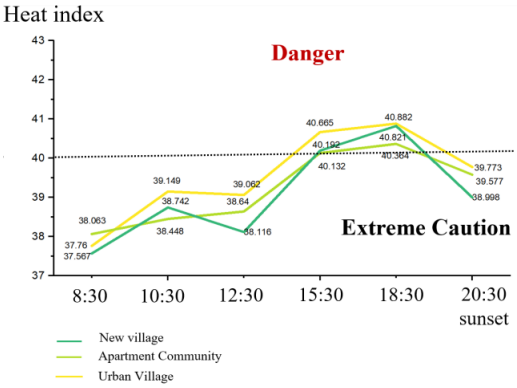

Figure 19 Average heat index level in three residential areas in 7th Aug

Currently, there is no specific metric for describing the density within urban villages. This study utilizes GIS methods to obtain data on building intervals in urban villages. Initially, by calculating the

difference between the building footprint and the total area of the region, the vacant land area within the region is determined. Utilizing GIS proximity analysis, the vacant land is segmented into multiple independent rectangular regions. Building interval data is then classified based on the length and width of these rectangular regions.

By correlating the building interval data with heat index data at three different times of the day, an analysis of the correlation between building intervals and heat index is established. The study discusses the relationship between the degree of isolation of buildings in high-density areas and the thermal risk. In order to quantify the relationship between the heat index and spatial layout, this study utilizes the average heat index values in urban and village areas during the testing period, as well as the inter-building spacing within blocks, to discuss their correlation. The magnitude of the Heat Index (HI) can be obtained through interval statistical calculations of data points in each grid location within local blocks using ArcGIS.

Based on three sets of data, the results in Fig.20 are obtained through correlation analysis. The analysis reveals that at different times of the day, the directional relationship between the heat index and building spacing varies. The building spacing is negatively correlated with HI at night, while building spacing is positively correlated with HI in the morning and noon.

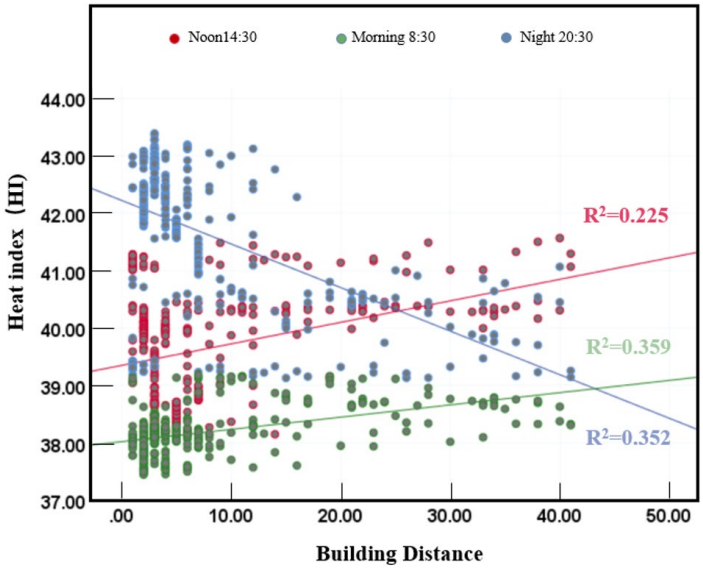

Figure 20 Relationships between heat index and building distance

The study conducted mobile observations in the Changban community of Guangzhou, examining the thermal environment at different times during summer heatwave events. This involved obtaining thermal environment parameters at multiple locations along the mobile route. Using a Heat Index (HI) model, the study focused on analyzing the spatiotemporal distribution of risks in urban villages, parks, apartment communities, and new villages during heatwaves. Spatial interpolation methods were employed to analyze the spatial characteristics of the HI during different testing periods, correlating the total average HI and basic spatial parameters to draw conclusions:

During heatwave events, urban villages exhibited the highest temperatures among all areas, with air temperatures consistently above 32 degrees Celsius. The peak temperatures were concentrated around noon at 2 o'clock, with the average air temperatures following the order: urban villages > apartment communities > new villages > parks. The temperature in new villages was the lowest among all residential areas, with the average air temperature inside the area about 1 degree Celsius lower than urban villages in the afternoon. The distribution of high and low values between local areas during heatwaves was distinctly contrasting.

Based on statistical analysis of building spacing parameters and correlation analysis between local block HI values, the correlation between building spacing and the Heat Index varied at different times. At noon, there was a negative correlation between building spacing and the HI, indicating higher heat risks in urban villages with denser building layouts. However, in the morning and evening, building spacing showed a positive correlation with the HI, suggesting that increasing

spacing could alleviate heat stress.

Comparing new villages with urban villages, controlling building spacing through artificial planning methods can effectively manage heat safety in the area. This study provides new insights for future urban village renovations and updates by controlling building spacing.

4. Published Paper etc.

[Underline the representative researcher and collaborate researchers]

[Published papers]

1. Haotian Wu, Qiong Li. Impact of Local Climate Zone Change on Urban Surface Heat Island intensity.Journal of Building Energy Efficiency, 2023,51(10):62-70. DOI:10.3969/j.issn.2096-9422.2023.10.009. (in Chinese)
2. Qiong Li, Qingrong Yang, Huiwang Peng, Chong Meng, Yuechao Deng. Spatial and Temporal Characteristics of High Temperature and Heat Waves along the “Belt and Road”. Journal of Building Energy Efficiency, 2023,51(10):54-61. DOI:10.3969/j.issn.2096-9422.2023.10.009. (in Chinese)

[Presentations at academic societies]

1. Speaker: **Qiong Li**. Title: The spatiotemporal variation characteristics of high-temperature heatwaves in the “Belt and Road” country. Conference: Special Live Broadcast on the Research, Development, and Application of Green Building Technologies and Standards in Countries Participating in the Belt and Road Initiative." ——Think-Tank-Forum Hosted by Journal of Building Energy Efficiency, Nov.11, 2023
2. Speaker: **Haotian Wu**. Title: the impact of urban development on surface heat island intensity. Conference: Special Live Broadcast on the Research, Development, and Application of Green Building Technologies and Standards in Countries Participating in the Belt and Road Initiative." ——Think-Tank-Forum Hosted by Journal of Building Energy Efficiency,Nov.11, 2023
3. Speaker: **Qiong Li**. Title: Research on urban thermal safety in the “Belt and Road” country. Conference: The 19th International Conference on Green Buildings and Building Energy Efficiency，May 15, 2023
4. Speaker: **Qiong Li**. Title: Study on the regional classification and risk assessment of heatwaves in China. Conference: Research Gathering Meeting of Wind Engineering Research Center of TPU，March 4, 2024

5. Research Group

1. Representative Researcher

Qiong Li (South China University of Technology)

2.Collaborate Researchers

1)Yingli Xuan (Tokyo Polytechnic University)

2)Haotian Wu (South China University of Technology)

3)Qinrong Yang (South China University of Technology)

6. Abstract (half page)

Research Theme
Representative Researcher (Affiliation)
Summary・Figures

This study is based on the past and current status of summer high-temperature heat waves in China, and it conducts research and analysis from multiple perspectives and scales. Firstly, based on the Crichton risk assessment framework, different indicators representing hazards, exposure, and vulnerability were selected to quantitatively analyze and generate a comprehensive heat wave risk index. Using spatial clustering methods, the characteristics of high-temperature heat waves in China were divided into zones, resulting in the delineation of six regions based on heat wave characteristics. Building on the heat wave zoning, actual observations were conducted in high-risk areas with dense populations.

Further, basing on the heat wave zoning, actual observations were conducted in high-risk areas with dense populations. The study conducted mobile observations in the Changban community of Guangzhou, examining the thermal environment at different times during summer heatwave events. This involved obtaining thermal environment parameters at multiple locations along the mobile route. Using a Heat Index (HI) model, the study focused on analyzing the spatiotemporal distribution of risks in urban villages, parks, apartment communities, and new villages during heatwaves. Spatial interpolation methods were employed to analyze the spatial characteristics of the HI during different testing periods, correlating the HI and basic spatial parameters to explore a new insight future urban village renovation.

Overall, Urban villages exhibited the highest temperatures among all regions, with air temperatures consistently exceeding 32 degrees Celsius. The peak occurred around 2:00 PM, and the average air temperature followed the order $T_{\text{Urban Village}} > T_{\text{Apartment Community}} > T_{\text{New Village}} > T_{\text{Park.}}$ All three types of residential areas experienced temperatures exceeding 40 degrees during the daytime. Urban villages exhibited the most adverse thermal conditions, with the heat index reaching the "dangerous" level for most of the daytime. Based on the statistical results of building spacing parameters and the correlation analysis between the local block Heat Index values, it is evident that the correlation between building spacing and the Heat Index varies at different times. The comparative results between new villages and urban villages suggest that the method of controlling building spacing through intentional planning can effectively manage thermal safety within a region.